ATLAS NOTE

ATL-COM-PHYS-2008-002

June 16, 2008

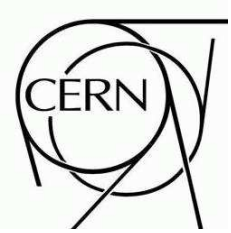

Heavy Quarkonia Perspectives with Heavy-Ions in ATLAS

L. Rosselet[1], P. Nevski[2], S. Timoshenko[3]

[1] University of Geneva, CH-1211 Geneva 4
[2] Brookhaven National Lab., Upton, NY 11973-5000
[3] Moscow Physics Engineering Institute, RU-115409 Moscow

Abstract

ATLAS will study a full range of observables and phenomena which characterize the hot dense medium formed in heavy-ion collisions, and in particular heavy quarkonia suppression which provides a handle on deconfinement mechanisms. As each quark-antiquark bound state is predicted to dissociate at a different temperature, the systematic measurement of the suppression of these resonances should provide some sort of thermometer of the early stage of the system evolution. We report on an evaluation of the ATLAS potential to measure resonances of the Υ and J/ψ families created in Pb+Pb collisions.

1 Introduction

Dissociation of heavy-flavor bosons is a very promising signature of QGP formation [1] that can potentially be studied with the ATLAS detector. This phenomenon is linked to the saturation of the long-range attractive potential in a QCD medium. Color screening effects prevent the various ψ, Υ, χ states from being formed when the color screening length becomes smaller than the size of the resonances. Thus, observation of the suppression of these states provides crucial tests of the nuclear potential.

The evidence for J/ψ suppression reported by the NA50 CERN experiment [2] at $\sqrt{s}$=17.3 GeV per nucleon pair and also by the PHENIX collaboration [3] at RHIC at $\sqrt{s}$=200 GeV raised a large interest for this kind of studies, although the interpretation is still a subject of debate, as the observed suppression results from a complex interplay between suppression and regeneration scenarios [4].

At the LHC, in addition to the J/ψ family, the Υ family will also be accessible, which will allow the study of c and b quarkonia states with a large variety of binding energies, and thus provide more powerful tests of screening effects in a saturated color potential.

The capability of observing quarkonia production in ATLAS, and their possible suppression in a hot dense deconfined medium, is the subject of this paper. Mainly decays of the resonances into muon pairs are considered, since these offer clear trigger and experimental signature. A study of the capability of observing Υ, $J/\psi \to e^+e^-$ and heavy-flavor production is also under way.

2 Methods to measure muons

As the standalone Muon Spectrometer provides an insufficient mass resolution (approximately 460 MeV) to separate the various states which dissolve at different temperatures inside the Υ and J/ψ families, muon candidates reconstructed in the Muon Spectrometer were matched to tracks in the Inner Detector (reconstructed using the information from the Pixels and SCT detectors [5]). The resulting combined mass resolution is mainly determined by the Inner Detector capability of measuring low-momentum tracks, and is limited by multiple scattering in the tracker material. However, the Muon Spectrometer is essential for trigger and muon identification purposes. Thus, two matching algorithms, using reconstructed tracks from the Inner Detector and Muon Spectrometer, were developed to get an optimal mass resolution. The first algorithm associates tracks fully traversing the Muon Spectrometer (3 muon stations) with Inner Detector tracks through a global fit. The second algorithm uses a tagging method which selects Inner Detector tracks whose extrapolation coincides with a track segment of the Muon Spectrometer. The advantage of the first technique is to reduce the contamination and to improve slightly the momentum resolution, whereas the second method reconstructs muons with a lower momentum threshold, as shown in Fig. 1, and which increases the acceptance for the J/ψ (Υ) typically by a factor up to 3.5 (1.5). In the first algorithm, the matching is done by a selection on the χ^2 of a global track fit between the different detectors, keeping the best combinations. In addition, a χ^2 cut and a geometrical $\Delta\phi \times \Delta\eta$ cut is applied, where $\Delta\phi$ and $\Delta\eta$ are the differences in azimuthal angle and pseudo-rapidity between Inner Detector tracks and Muon Spectrometer tracks after back-extrapolation to the vertex. The quality of the matching can be deduced from Figs. 2 and 3, while Fig. 4 shows the χ^2 of the best association. For further analysis, a set of rather loose selection cuts was chosen, namely a geometrical cut $R = \sqrt{\Delta\phi^2 + \Delta\eta^2} < 0.25$ and a cut $\chi^2 < 5$. The second algorithm is applied after the first algorithm and concerns tracks traversing only 2 muon-stations out of 3 normally. The association is done by comparing the positions ϕ_{pos}, η_{pos} and the angles ϕ, η at the entrance of the Muon Spectrometer between extrapolated Inner Detector tracks and Muon Spectrometer track segments. The quality of the matching can be seen in Fig. 5. For further analysis, rather loose geometrical cuts are applied: $R_{pos} = \sqrt{(\Delta\phi_{pos}/a)^2 + (\Delta\eta_{pos}/b)^2} < 1$ and $R_{angle} = \sqrt{(\Delta\phi/c)^2 + (\Delta\eta/d)^2} < 1$ with a=0.07 (0.10), b=0.20 (0.20), c=0.25 (0.30) and d=0.25 (0.25) for Υ (J/ψ) studies, respectively.

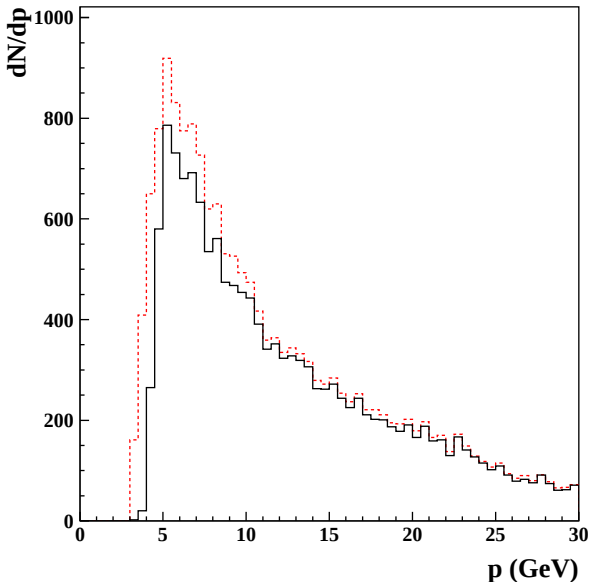

Figure 1: Momentum distribution for reconstructed muons from ϒ decays with the matching algorithm based on a global fit (full line) and with the algorithm based on a tagging method (dashed line).

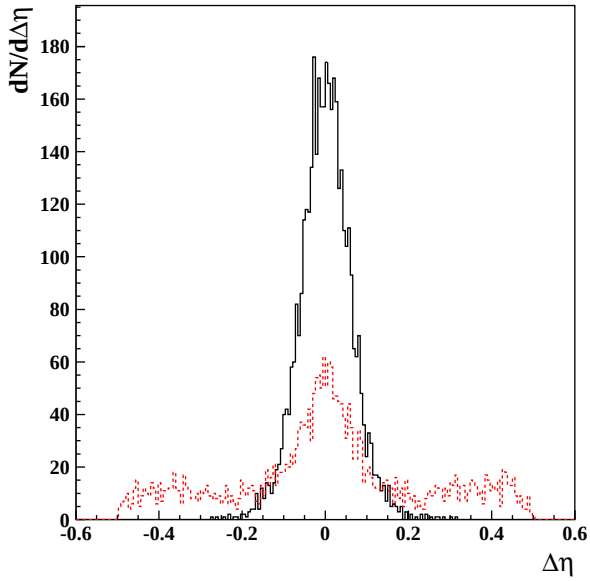

Figure 2: Pseudo-rapidity difference between tracks reconstructed in the Inner Detector and in the Muon Spectrometer after back-extrapolation to the vertex, for muons from ϒ decays (full line) and from central HIJING events (dashed line).

As the first algorithm provides a more stringent muon selection than the second one, all di-muons used in the present study were chosen with at least one muon reconstructed with the first algorithm, ending up with two selections of di-muon pairs: the ”Global Fit” selection with both muons reconstructed with the first algorithm, and the ”Global+Tag” selection with at least one muon from the first algorithm,

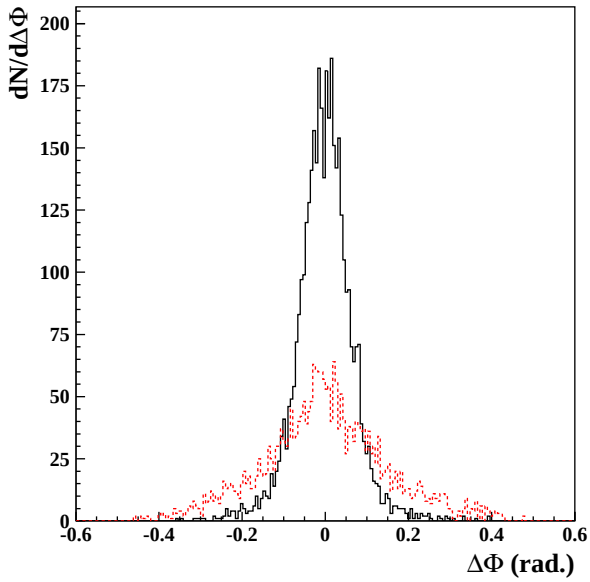

Figure 3: Azimuthal angle difference between tracks reconstructed in the Inner Detector and in the Muon Spectrometer after back-extrapolation to the vertex, for muons from ϒ decays (full line) and from central HIJING events (dashed line).

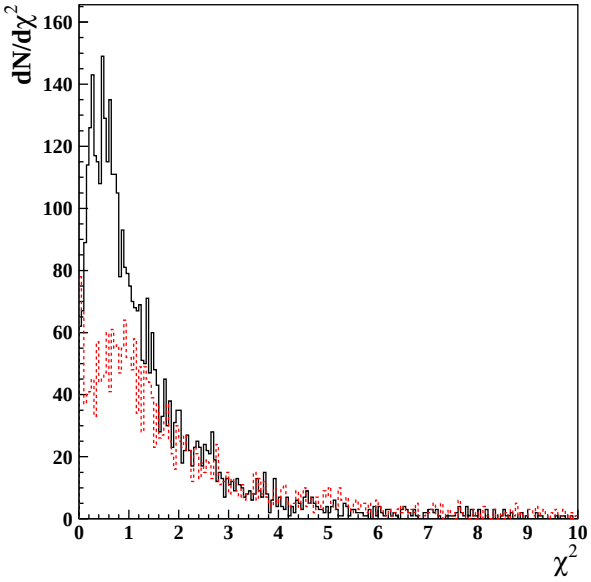

Figure 4: χ^2 distribution of the global track fit for muons from ϒ decays (full line) and from central HIJING events (dashed line) .

the second muon coming from either algorithm. The choice between these two strategies is basically a trade off between statistics and purity with little effect on mass resolution.

An additional way to increase the heavy quarkonia statistics is to reduce the toroidal field of the Muon Spectrometer as it improves the low p_T muon acceptance. It has also the advantage to make easier

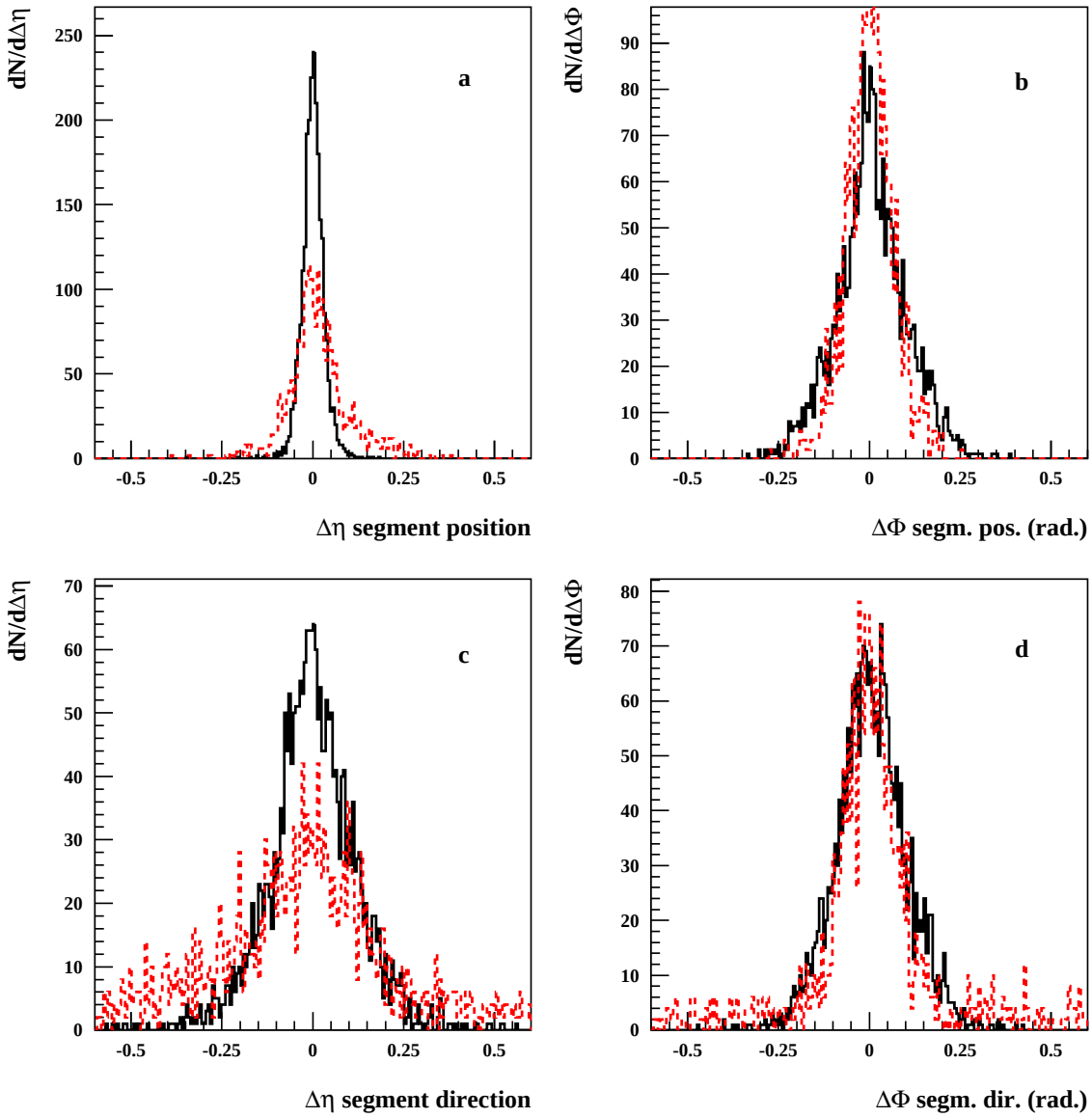

Figure 5: Pseudo-rapidity and azimuthal angle difference of positions (a, b) and directions (c, d) at the entrance of the Muon Spectrometer between extrapolated Inner Detector tracks and Muon Spectrometer track segments for the best association with the tagging algorithm. The full lines are for reconstructed muons from Υ decays and the dashed lines for muons from central HIJING events.

a low p_T muon trigger (see Section 7) but at the expense of a worse mass resolution. Four different studies were made using either the "Global Fit" or the "Global+Tag" selection with the standard setting of the field ($\int Bdl = 4$ Tm) and half field ("B/2 mode") in the toroidal magnet of the Muon Spectrometer. A possibility to improve the mass resolution and to compensate the loss due to the field reduction, would be to use the Transition Radiation Tracker, if the charged multiplicity allows it. The best compromise between these different strategies depends mainly on the real charged multiplicity, which is difficult to

predict for heavy-ion collisions at the LHC energy.

3 Upsilon generation, acceptance and reconstruction

The intrinsic di-muon mass resolution of the ATLAS detector was studied with single Υ decays into muon pairs. A first sample of 30000 $\Upsilon \rightarrow \mu^+\mu^-$ events were generated with PYTHIA. These events were then processed through the GEANT3 full simulation, and reconstructed with the ATLAS Muon Spectrometer reconstruction package Muonbox [5], the Inner Detector reconstruction package xKalman (package ATLSIM 7.5.0), and with specially developed algorithms for the association of Muon Spectrometer and Inner Detector tracks as discussed in the previous Section. These results have been partially cross checked using the ATLAS package ATHENA 12.0.6, based on GEANT4 full simulation, as explained at the end of this Section.

In addition to the geometrical cut explained in the previous Section, a cut on the muon transverse momentum $p_T > 3$ GeV was applied. Figures 6 and 7 show the transverse momentum and rapidity distributions dN/dp_T and dN/dy of the $\Upsilon \rightarrow \mu^+\mu^-$. The generated distributions are in black whereas the reconstructed distributions are in red for the "Global Fit" and in blue for the "Global+Tag" strategies with the full field. Even with a muon transverse momentum cut $p_T > 4$ GeV (green line), the full Υ p_T range is covered. The two-peak structure of the reconstructed distributions with $p_T > 3$ GeV in Fig. 7 is due to the p_T-rapidity correlation at low p_T. Figure 8 and the two first lines of Table 1 show the di-muon mass resolution and the (integrated) event acceptance and reconstruction efficiency after selection, as a function of the pseudo-rapidity cut on the decay muons (see Sections 3 and 5 for comments on the impact of the HIJING background and on the B/2 mode). It is clear that a compromise has to be found between the overall rate of accepted events and the mass resolution, which vary in opposite directions when the pseudo-rapidity acceptance of the decay muons increases, in order to separate Υ from Υ' in a clean way and with maximum statistics. Typically, in the Υ mass region, limiting the muon acceptance to $|\eta| < 1.75$-2, according to the strategy used, would provide a mass resolution below 150 MeV, sufficient to separate Υ and Υ' states, as can be appreciated from the plot in Fig. 8. The separation between Υ' and Υ'' is more difficult to achieve, but less important as these two resonances have a rather similar dissociation temperature ($\sim T_c$, the temperature of transition to QGP), contrary to the Υ whose dissociation temperature is quite higher ($2.3 \times T_c$) [6]. Such a clear separation is not achievable in the forward regions. Further studies are however needed to optimise the muon pseudo-rapidity acceptance.

A few additional checks were performed. With only two Pixel layers, as forseen in the initial (staged) layout of the Inner Detector, the mass resolution improved slightly because of the smaller amount of material. Applying even looser selection cuts than those described above, i.e. $R < 0.5$, $\chi^2 < 10$ and $p_T > 1.5$ GeV, increases the acceptance only slightly, namely to 14.6% (2.86%) instead of 12.0% (2.64%) for the full detector (central part).

Finally the acceptance and efficiency values quoted in Table 1 have been cross checked using ATHENA, release 12.0.6, for 30000 $\Upsilon \rightarrow \mu^+\mu^-$ events with full field. The matching between the Inner Detector and the Muon Spectrometer tracks was done using the package STACO with some additional cuts: a geometrical cut $R < 0.25$, a cut on the muon-$p_T > 3$ GeV and a cut $\chi^2 < 34$. The results were found to be similar with a combined acceptance and efficiency of 12.8% (2.58%) for the full detector (central part), as compared to 12.0% (2.64%) obtained with ATLSIM 7.5.0 for the "Global Fit" selection. The results of the comparison are shown in Table 1.

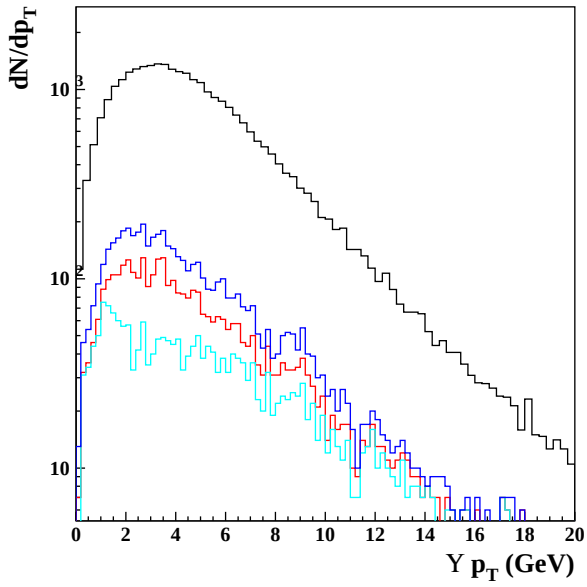

Figure 6: dN/dp_T distribution for $\Upsilon \to \mu^+\mu^-$ (color online). The generated distribution is in black, the reconstructed distribution is in green for the "Global Fit" selection with a muon-p_T >4 GeV, in red for the "Global Fit" selection with a muon-p_T >3 GeV, and in blue for the "Global+Tag" selection with a muon-p_T >3 GeV.

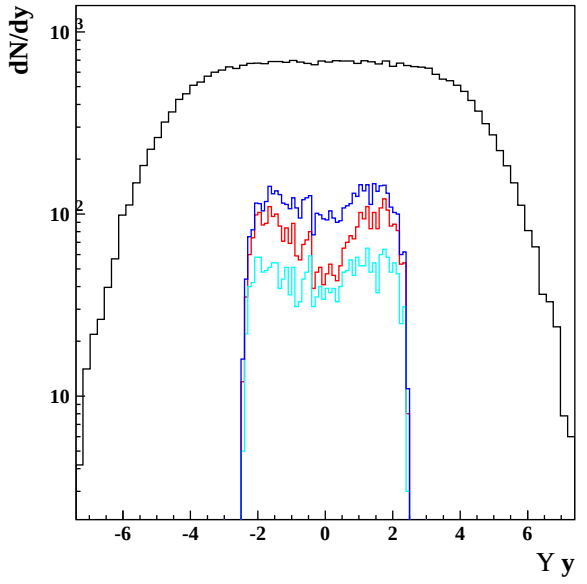

Figure 7: dN/dy distribution for $\Upsilon \to \mu^+\mu^-$ (color online). The generated distribution is in black, the reconstructed distribution is in green for the "Global Fit" selection with a muon-p_T >4 GeV, in red for the "Global Fit" selection with a muon-p_T >3 GeV, and in blue for the "Global+Tag" selection with a muon-p_T >3 GeV.

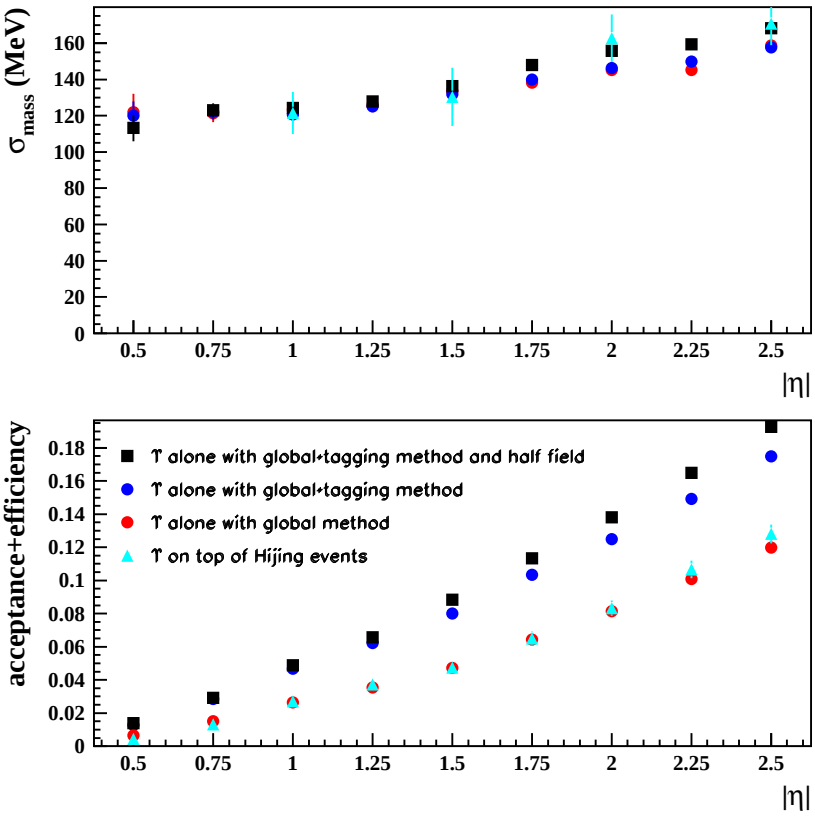

Figure 8: The ϒ mass resolution (top) and the integrated ϒ selection efficiency after cuts (bottom), as a function of the pseudo-rapidity acceptance of the decay muons for different strategies. Results for isolated ϒ and for ϒ embedded in HIJING central events are shown with the "Global Fit" method and full field. A comparison between "Global Fit" and "Global+Tag" selections with full field, as well as a comparison between full and half field with the "Global+Tag" strategy are also displayed (see text).

4 Background studies

Background events, generated using HIJING 1.38, were processed through a full GEANT3 simulation, and were reconstructed with the tools described in the previous Section. This detailed simulation makes sure that local high multiplicities and possible detector saturation effects are taken into account. A total of 5000 central (b <1 fm) Pb+Pb collisions were produced.

Most of the muons in these background events come from in-flight decays (i.e. before absorption in the calorimeters) of π and K (indirect muons), and from c and b decays directly at the vertex (direct muons). The direct muons have on average a larger p_T than the indirect ones, therefore the ratio of direct/indirect muons depends on the p_T cut used in the analysis. Because secondary tracks from particles decaying away from the initial vertex usually produce kinks, geometrical and χ^2 cuts, in addition to p_T cuts, are quite efficient to suppress indirect muons. This is illustrated in Figs. 2 and 3. These plots were made for all muon candidates with R <0.5 after the global fit of the first matching algorithm, and can be compared with the distributions obtained in very similar conditions for the ϒ signal. The latter (full line) show cleaner matching properties than the former (dashed line), thanks to the absence of π/K decays. Figures 9 and 10 show the p_T and pseudo-rapidity distributions of the reconstructed muons

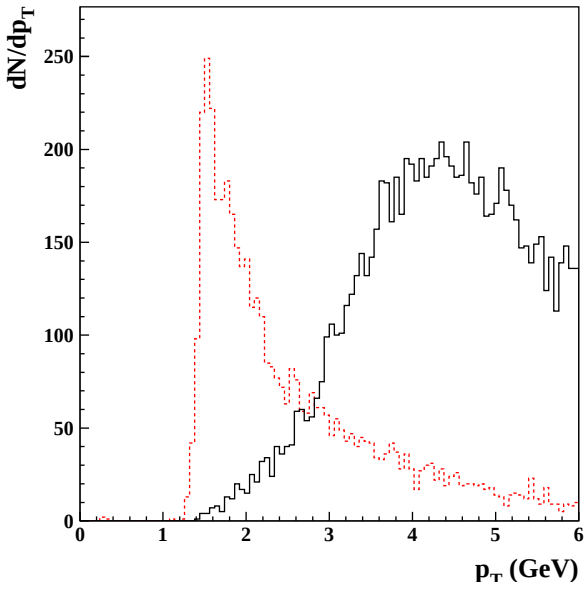

Figure 9: Transverse momentum distribution for reconstructed muons from Υ decays (full line) and from central HIJING events (dashed line).

(dashed line). Again, these distributions are quite different from those obtained for muons from Υ decays (full line). In particular, a p_T cut in the 3-3.5 GeV range is quite effective to separate the Υ signal from the background. The two peaks at large $|\eta|$ in Fig. 10 are due to low-p_T muons, and are considerably reduced after a p_T >3 GeV cut is applied.

After the selection cuts described in the previous Section are applied to this background sample, the number of reconstructed muons with the global fit is reduced to 0.21 (0.48) muons per event on average for p_T >3 GeV (p_T >1.5 GeV). Compared to the number of muons initially reconstructed in the Muon Spectrometer alone, 0.94 per central HIJING event over $|\eta|$ <2.5, the background muons after these cuts are reduced by a factor 4.4, due to the 3 GeV p_T cut, the matching to tracks and the track reconstruction efficiency in the Inner Detector.

The fraction of direct muons in the sample surviving the above-mentioned set of cuts was found to be 35%, increasing to 46% if the geometrical cut is tightened from R <0.25 to R <0.1. The background after cuts is therefore still dominated by π and K decays.

It was also checked that the global fit associates correctly the muon track found in the Muon Spectrometer to an Inner Detector track coming from a direct or indirect muon. This is the case for 91% (74%) of the μ candidates with $|\eta|$ <1 ($|\eta|$ <2.5) passing the above selections, and for 97% (89%) of the candidates passing a tightened R <0.1 geometrical cut.

At this stage an additional geometrical cut was applied on the di-muon candidates: the distance between both reconstructed muons at the vertex must be below 0.02 cm (0.04 cm) in the Υ (J/ψ) analysis. This cut reduces the surviving background (see Fig. 11), whereas the loss in Υ (1.6%) and J/Ψ (1.7%) is negligible.

The average number of reconstructed $\mu^+\mu^-$ pairs per central event was found to be 0.012 for the "Global Fit" selection and 0.020 for the "Global+Tag" selection with a muon-p_T cut at 3 GeV. This includes both correlated and uncorrelated muon pairs. No cut on the di-muon invariant mass has been applied at this stage. Such a cut might be applied at the high level trigger.

Due to the small statistics of surviving muons, the shape of the di-muon mass distribution for the

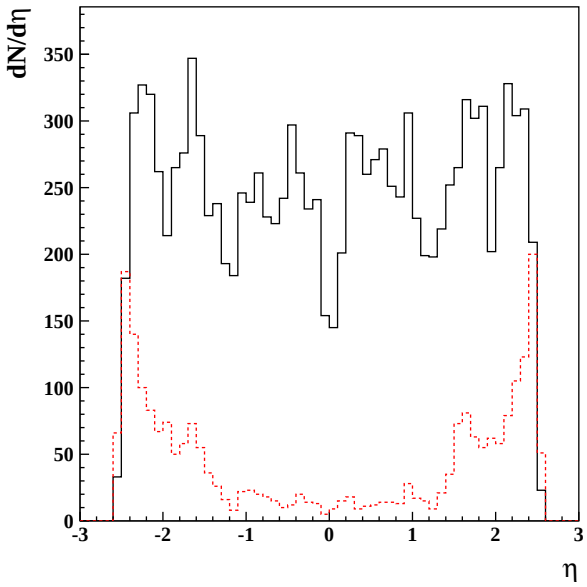

Figure 10: Pseudo-rapidity distribution for reconstructed muons from Υ decays (full line) and from central HIJING events (dashed line).

background sample was obtained with a mixed-event technique, where the two muons were taken from two different events. As a consequence, this method provides only the mass shape of uncorrelated muon pairs. The result is shown in Fig. 12.

The capability of reconstructing Υ decays in complete heavy-ion events was studied by merging the two samples discussed in the previous Section, namely single $\Upsilon \to \mu^+\mu^-$ events and central Pb+Pb HIJING events.

Figures 13 and 14 show the reconstructed $\mu^+\mu^-$ invariant mass distribution for a sub-sample of these combined events. The Υ mass resolution was found to be 170.7±11.8 MeV for muons inside the full acceptance ($|\eta|$ <2.5), and 121.5±11.6 MeV for muons with $|\eta|$ <1. Comparing these mass resolutions to those obtained for single Υ events (see Fig. 8 and Section 3), one can see that the performance is only slightly affected by the presence of the heavy-ion background. The signal purity in the mass region 9.1-9.8 GeV defined as the fraction of muon pairs with both muons coming from the Υ, is 94% for the standard analysis with the "Global Fit" selection and 96% for muons with $|\eta|$ <1. These values do not take into account the Υ' contamination in the Υ mass region.

The results obtained with the merged events (represented by triangles in Fig. 8) have been used to estimate production rates and signal-to-background ratios.

5 Production rates and signal-to-background ratio

The $\Upsilon \to \mu^+\mu^-$ cross-section at the LHC energies can be estimated by linear extrapolation of the CDF data from $\sqrt{s}$=1.8 TeV [7] to $\sqrt{s}$=5.5 TeV. The extension from $p\overline{p}$ collisions to AA collisions is then obtained by using the A-scaling law

$$\left[\frac{d\sigma(AA)}{dy}\right]_{y=0} = A^{2\alpha}\left[\frac{d\sigma(p\overline{p})}{dy}\right]_{y=0} \quad (1)$$

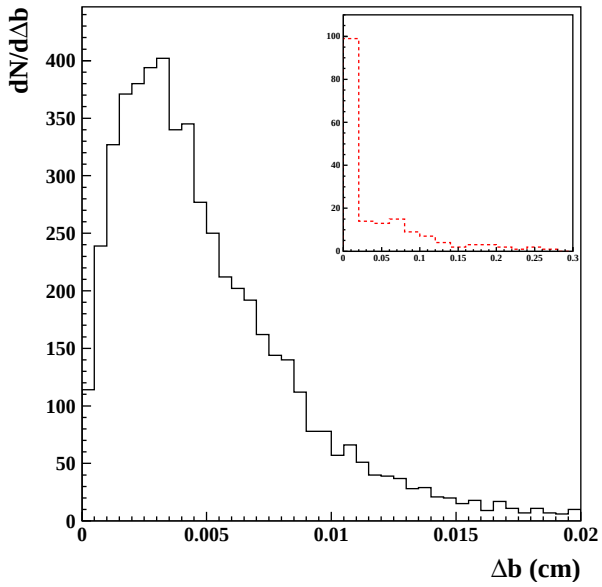

Figure 11: Distance at the vertex between both reconstructed muons for Υ decays (full line) and for background muon pairs from central HIJING events in the inset (dashed line).

with α=0.95 for the b-states [8]. Values of cross-section times branching ratio of $B_r d\sigma/dy(Pb+Pb \rightarrow \Upsilon \rightarrow \mu^+\mu^-)$=304 μb, $B_r d\sigma/dy(Pb+Pb \rightarrow \Upsilon' \rightarrow \mu^+\mu^-)$=78 μb, and $B_r d\sigma/dy(Pb+Pb \rightarrow \Upsilon'' \rightarrow \mu^+\mu^-)$= 44.4 μb have been used [9], where B_r indicates the branching ratios for Υ, Υ' and Υ'' decays into muon pairs. These cross-sections are valid for minimum-bias Pb+Pb collisions.

In these studies, the signal-to-background ratio S/B has been estimated starting from the average number of reconstructed $\mu^+\mu^-$ pairs per central HIJING events, i.e. 0.020 with the standard set of cuts and the "Global+Tag" selection. Since the di-muon background is expected to be proportional to N^2, the square of the charged particle multiplicity above the applied p_T cut, a correction factor $(N_{b=0}/N_{min-bias})^2$ was used to derive the $\mu^+\mu^-$ background for minimum-bias events from that determined in Section 1.3 for central Pb+Pb collisions. With $N_{b=0}/N_{min-bias}$=4.75, the expected number of $\mu^+\mu^-$ pairs per event is $\sim 8.9 \times 10^{-4}$. Taking into account the signal and background acceptances in the Υ mass region, and assuming a total Pb+Pb cross-section of 8 b and a $\Upsilon \rightarrow \mu^+\mu^-$ production cross-section of 304 μb, signal-to-background ratios of S/B =0.2 and S/B =0.3 were obtained over the full detector acceptance and for the region $|\eta|$ <1 respectively, with the "Global+Tag" selection.

The detailed results of S/B ratios and of the significance $S/\sqrt{S+B}$ of the "Global Fit" and of the "Global+Tag" strategies are shown in Table 1 for the nominal setting of the toroidal field and for the B/2 mode. For the Υ family, where the limiting factor is the mass resolution needed to separate the states, no improvement in statistics is expected for a given resolution with the B/2 mode, as the acceptance-to-resolution ratio is about similar as in the case of the nominal field setting (see Fig. 8).

These estimates have to be taken with caution, and need to be confirmed by more complete studies based on high-statistics samples of minimum-bias Pb+Pb events. The background level depends crucially on the maximum charged particle multiplicity given by the generator, especially in the forward regions. It is also very sensitive to the π and K transverse momentum distributions used in the model. As an example, with the SHAKER generator, which predicts a harder p_T spectrum for pions and kaons than HIJING, the estimated S/B ratio would decrease by about a factor two [10].

On the other hand, these studies have been made with algorithms not specially tuned to the heavy-ion

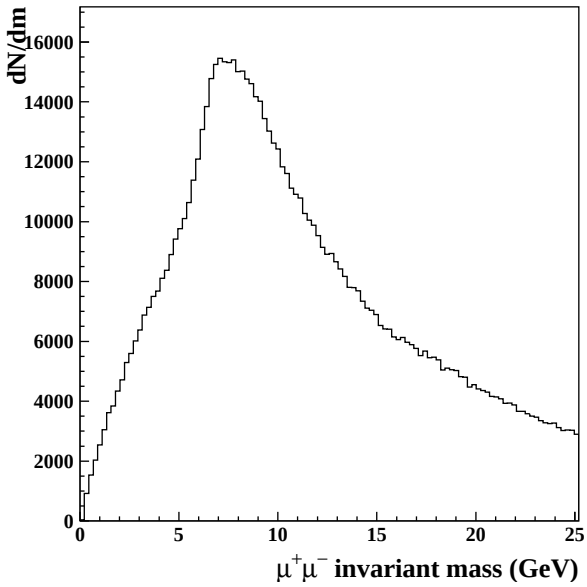

Figure 12: Reconstructed di-muon mass spectrum for muons from central HIJING events, as obtained with a mixed-event technique (see text).

environment, and with simple analysis cuts and techniques. There is therefore margin for improvement.

The number of $\Upsilon \to \mu^+\mu^-$ events which can be accumulated in one month of Pb+Pb operation has been estimated by assuming 10^6 s of effective data taking time, which corresponds to a machine and experiment efficiency of 40%. Assuming an average luminosity of 0.4×10^{27} cm^{-2} s^{-1}, and a signal acceptance limited to 8% by a muon pseudo-rapidity cut $|\eta| < 2$ (in order to get a clean separation between Υ and Υ'), the number of events after background subtraction is expected to be $\geq 10^4$ per month of Pb+Pb running, which corresponds to an integrated luminosity of 0.4 nb^{-1}. This number does not take into account the trigger efficiency which has not been applied at this stage. Nevertheless, even assuming an additional signal reduction by a factor of two, to account for inefficiencies from the trigger and/or additional analysis cuts, the remaining statistics will hopefully be sufficient to study the Υ production as a function of p_T for collisions with different centralities.

Fig. 15 shows the $\mu^+\mu^-$ invariant mass distribution in the Υ region for a muon pseudo-rapidity cut $|\eta| < 2$ without background, and with background in the inset, as expected for a month of data taking.

The Transtion Radiation Tracker (TRT) has not been considered for this study because of its large occupancy in central Pb+Pb collisions. Nevertheless the TRT can be used fully if the charged multiplicity is low enough as in peripheral collisions, and at least partially in central Pb+Pb collisions. This should improve tracking and resolution. The TRT can also be used to identify low p_T electrons and to study Υ and $J/\psi \to e^+e^-$. An evaluation of the potential of the TRT as a function of the charged multiplicity is under way.

Suppression of quarkonia resonances has to be established with respect to a signal which is not affected by the evolution of the interacting coloured medium created in the Pb+Pb collision. At the LHC the Drell-Yan process, which was used as a reference at the SPS [2], is expected to have a very low rate. The possibility of using $Z^0 \to \mu^+\mu^-$ decays, and maybe also $Z^0 \to e^+e^-$, is being investigated.

Field	full	full	full	half	half	half
$\|\eta\|$ (max)	1	2	2.5	1	2	2.5
Acceptance x efficiency	4.7%	12.5%	17.5%	4.9%	13.8%	19.3%
	(2.6%)	(8.1%)	(12.0%)	(2.6%)	(8.9%)	(13.4%)
Cross check using ATHENA	2.6%	8.3%	12.8%			
Mass resolution (MeV)	123	145	159	126	162	176
S/B	0.3	0.2	0.2	0.3	0.2	0.2
	(0.4)	(0.3)	(0.3)	(0.55)	(0.3)	(0.3)
$S/\sqrt{S+B}$	37	46	55	37	50	60
	(31)	(45)	(55)	(34)	(48)	(60)
Signal rate/month	5700	15000	21200	5900	16800	23400
	(3100)	(10000)	(14600)	(3100)	(10800)	(16300)

Table 1: Total acceptance and reconstruction efficiency, mass resolution, signal-to-background ratio S/B, significance $S/\sqrt{S+B}$ and expected rates as a function of the maximum pseudorapidity cut on the decay muons of $\Upsilon \to \mu^+\mu^-$ with a muon-p_T >3 GeV for the "Global+Tag" selection and two settings of the toroidal field (nominal and B/2 mode). The results for the "Global Fit" selection are in parenthesis. The mass resolution is equivalent with both selections. The results from ATHENA 12.0.6 are also shown for comparison with the "Global Fit" selection results.

Field	full	full	half
p_T (min) (GeV)	3	1.5	1.5
Acceptance x efficiency	0.055%	0.530%	1.100%
	(0.039%)	(0.151%)	(0.529%)
Cross check using ATHENA	0.034%	0.192%	
Mass resolution (MeV)	68	68	76
S/B	0.4	0.15	0.15
	(0.5)	(0.2)	(0.25)
$S/\sqrt{S+B}$	56	113	164
	(52)	(72)	(140)
Signal rate/month	11000	104000	216000
	(8000)	(30000)	(104000)

Table 2: Total acceptance and reconstruction efficiency, mass resolution, signal-to-background ratio S/B, significance $S/\sqrt{S+B}$ and expected rates as a function of the minimum p_T cut on the decay muons of $J/\psi \to \mu^+\mu^-$ for the "Global+Tag" selection and two settings of the toroidal field (nominal and B/2 mode). The results for the "Global Fit" selection are in parenthesis. The mass resolution is equivalent with both selections. The results from ATHENA 12.0.6 are also shown for comparison with the "Global Fit" selection results.

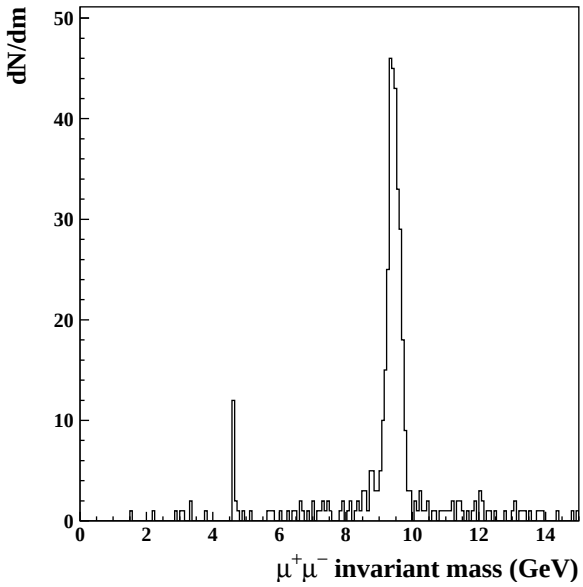

Figure 13: Reconstructed di-muon invariant mass distribution for Υ events embedded in central Pb+Pb events in the region $|\eta| < 2$.

6 Charmonium states

A basic difference in the experimental study of Υ and J/ψ production is that, because of its mass, the Υ can be measured over its full p_T spectrum starting at p_T=0 and η=0. Indeed, even if the Υ is produced at rest, the decay muons have in general enough energy to traverse the calorimeters and reach the Muon Spectrometer. The situation is different for muons from J/ψ decays, which in most cases need an additional p_T from the parent particle, or a Lorentz-boost, to reach the Muon Spectrometer. As a consequence, a full p_T analysis of the $J/\psi \rightarrow \mu^+\mu^-$ channel (which is important because quarkonia suppression may depend on the resonance transverse momentum) is only possible in the forward regions where, however, the background is largest.

On the other hand, the $J/\psi \rightarrow \mu^+\mu^-$ production has a much larger cross-section than Υ production, which allows stricter cuts to be applied to reduce the background. The cross-section for the process $J/\psi \rightarrow \mu^+\mu^-$ at the LHC can be derived, in a similar way as for the Υ, from Equation 1 with α=0.90, which gives $B_r d\sigma/dy(Pb+Pb \rightarrow J/\psi \rightarrow \mu^+\mu^-)$=49 mb and $B_r d\sigma/dy(Pb+Pb \rightarrow \psi' \rightarrow \mu^+\mu^-)$=879 μb [9].

Another advantage is that the reconstructed di-muon mass resolution ($\sim$70 MeV from a full-simulation study) is sufficient to separate J/ψ from ψ' even in the forward regions of the detector, which is not the case for the Υ resonances.

A first sample of 180000 single $J/\psi \rightarrow \mu^+\mu^-$ events were generated with PYTHIA, processed through the GEANT3 full simulation and analysed in the same way as the $\Upsilon \rightarrow \mu^+\mu^-$ sample. The dN/dp_T and dN/dy distributions for the $J/\psi \rightarrow \mu^+\mu^-$ are displayed in Fig. 16 and Fig. 17. The generated distributions are in black, the reconstructed distributions are in red for the "Global Fit" strategy with a muon-p_T >3 GeV, in green with a muon-p_T >1.5 GeV, and in blue for the "Global+Tag" strategy with a muon-p_T >1.5 GeV. The full lines are for the nominal setting of the toroidal field whereas the dashed lines are for half of the field. Due to the low mass of the J/ψ, the acceptance is mainly for $|\eta|$ >1.5, and the low p_T range is not accessible for a muon-p_T cut at 3 GeV as used for the Υ. On the

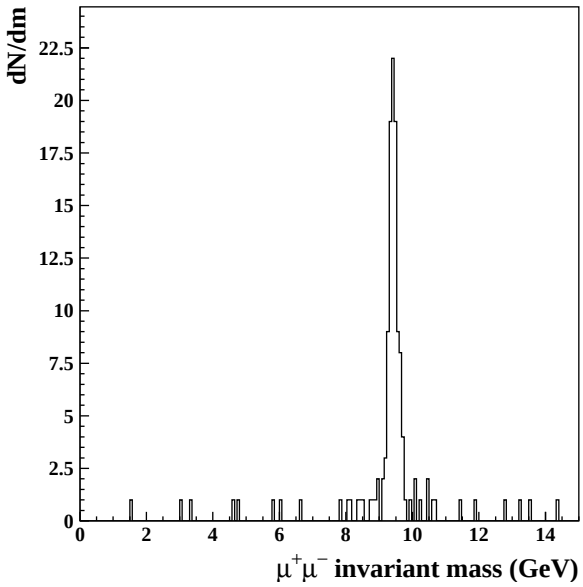

Figure 14: Reconstructed di-muon invariant mass distribution for ϒ events embedded in central Pb+Pb events in the region $|\eta| < 1$.

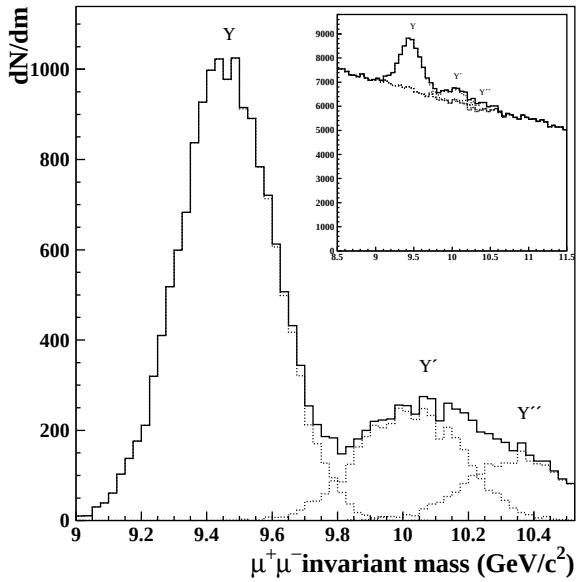

Figure 15: Di-muon invariant mass distribution for muons with $|\eta| < 2$ in the ϒ region without background, and with background in the inset.

contrary, with a muon-p_T cut at 1.5 GeV, the J/ψ can be measured from p_T=0. The strong correlation p_T-rapidity is visible in Fig. 18 for the J/ψ, and in Fig. 19 for the decay muons. A minimum energy of 3-4 GeV is needed for the muon to reach the Muon Spectrometer, corresponding to a p_T of 3-4 GeV at η=0. A Lorentz-boost is necessary for a muon-p_T of 1.5 GeV.

The detailed results of acceptance and reconstruction efficiency, mass resolution, signal-to-background

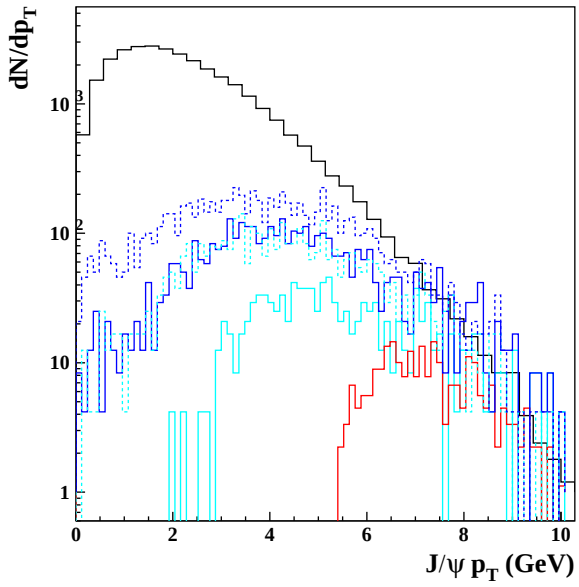

Figure 16: dN/dp_T distribution for $J/\psi \to \mu^+\mu^-$ (color online). The generated distribution is in black, the reconstructed distribution (x 25) is in red for the "Global Fit" selection with a muon-p_T >3 GeV, in green for the "Global Fit" selection with a muon-p_T >1.5 GeV and in blue for the "Global+Tag" selection with a muon-p_T >1.5 GeV. The full lines are for the nominal toroidal field in the Muon Spectrometer whereas the dashed lines are for half of the field.

ratio S/B, significance $S/\sqrt{S+B}$ and expected signal rates are displayed in Table 2. The "Global+Tag" selection with a muon-p_T >1.5 GeV increases substantially the significance. Depending on the strategy used, the number of $J/\psi \to \mu^+\mu^-$ events expected in one month of 0.4 nb^{-1} of integrated luminosity of Pb+Pb running ranges after background subtraction between 3 x 10^4 and 2 x 10^5 for a muon-p_T cut >1.5 GeV. The choice of the strategy is therefore more important for the J/ψ than for the Υ. A study of a trigger based on a low muon-p_T cut for $|\eta|$ >1.5 GeV is under way.

Concerning the results of the B/2 mode, the mass resolution is 15% worse, but the acceptance is 2-3 times better than with the nominal setting of the toroidal field. The significance is also much better. An equivalent acceptance times efficiency, but with a better S/B and significance, is obtained in the case of the "Global Fit, B/2 mode" compared to the "Global+Tag, full field" strategy. As the trigger is easier with the "Global Fit" method because both muons are fully traversing the Muon Spectrometer, this would support the B/2 mode, although other consequences have first to be carefully taken into consideration. Fig. 20 shows the reconstructed $\mu^+\mu^-$ invariant mass distribution in the J/ψ region for the "Global+Tag" selection, with a muon-p_T >1.5 GeV and full toroidal field, as expected for a month of data taking.

The acceptance and efficiency values quoted in Table 2 have been cross checked using ATHENA, release 12.0.6, for 164000 $J/\psi \to \mu^+\mu^-$ events with full field. The matching between the Inner Detector and the Muon Spectrometer tracks was done using the package STACO with the same additional cuts as described in Section 3 for the upsilons. The results were found to be similar for a muon-p_T >3 GeV and are also shown in Table 2. When reducing the muon-p_T cut to 1.5 GeV, the better efficiency obtained with ATHENA compared to ATLSIM is mainly due to a code optimized for low p_T track reconstruction in the Inner Detector.

Finally, it should be noted that tagging displaced vertices provides a tool to discriminate prompt J/ψ from B-meson decays. The ratio between prompt and decay J/ψ could be studied as a function of the

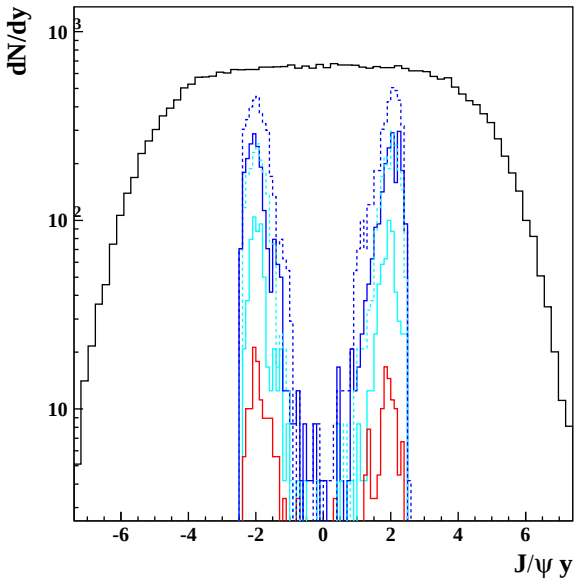

Figure 17: dN/dy distribution for $J/\psi \to \mu^+\mu^-$ (color online). The generated distribution is in black, the reconstructed distribution (x 25) is in red for the "Global Fit" selection with a muon-p_T >3 GeV, in green for the "Global Fit" selection with a muon-p_T >1.5 GeV and in blue for the "Global+Tag" selection with a muon-p_T >1.5 GeV. The full lines are for the nominal toroidal field in the Muon Spectrometer whereas the dashed lines are for half of the field.

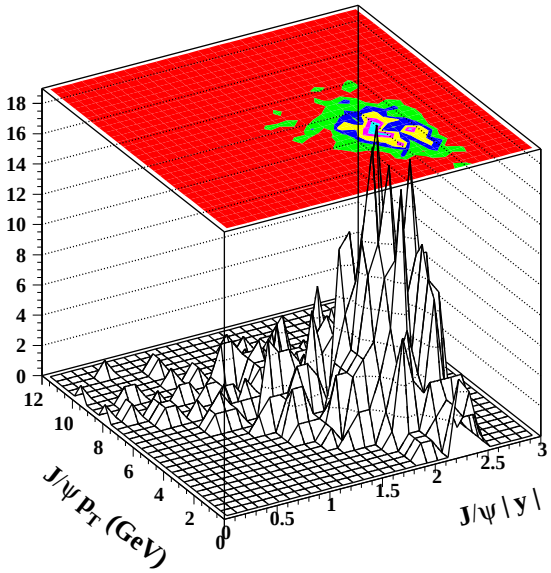

Figure 18: Two-dimensional spectrum as a function of the two variables p_T and $|y|$ of reconstructed J/ψ mesons.

event centrality.

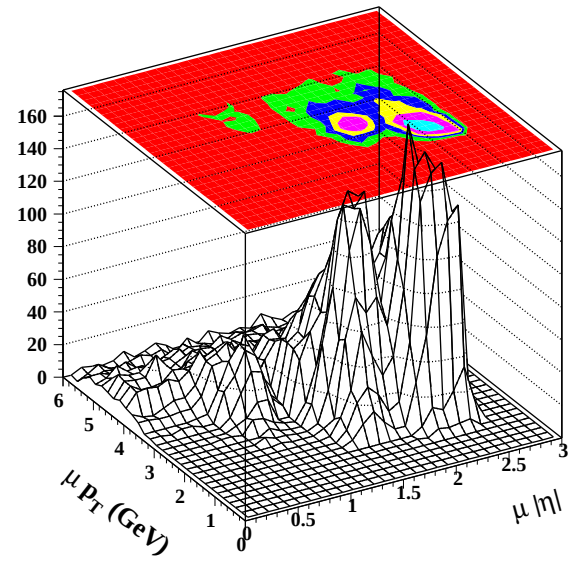

Figure 19: Two-dimensional spectrum as a function of the two variables p_T and $|y|$ of reconstructed muons from J/ψ decays.

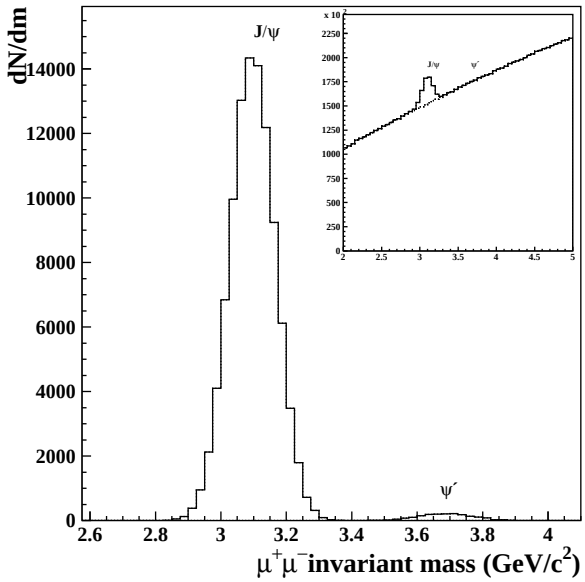

Figure 20: Di-muon invariant mass distribution in the J/ψ region without background, and with background in the inset.

7 Di-muon trigger

Possible schemes to trigger on Υ and $J/\psi \to \mu^+\mu^-$ events in heavy-ion collisions are presently being investigated. It is crucial to trigger on muons with p_T as low as 3-4 GeV for the Υ and even $\sim$1.5 GeV for the J/ψ, a possibility which is under study. The best option seems to combine an interaction trigger

with a loose di-muon trigger in the Muon Spectrometer.

The standard di-muon trigger for pp running has three levels. The first one is based on information from the muon-trigger chambers, provides a rough p_T cut and defines "Regions of Interest" [5], whereas level 2 is based on fast reconstruction inside the "Regions of Interest" preceedingly defined and level 3 has access to the entire event. The level 1 trigger, which is not designed for a low p_T muon trigger, can nevertheless provide an effective low p_T cut either by programming it to use only the ϕ plane information from the trigger chambers (almost no p_T cut as the bending is in η), or by reducing sufficiently the field in the toroidal magnet. It should be noted that, even if the event reduction provided by such a level 1 trigger is limited by the background, the maximum interaction rate in Pb+Pb running ($\sim$8 kHz for a luminosity of 10^{27} cm^{-2} s^{-1}) is already one order of magnitude lower than the maximum output rate of the level 1 trigger forseen in pp at designed luminosity.

The challenge will be then to define levels 2 and 3 of the di-muon trigger sufficiently selective to reduce the data taking to an acceptable rate (ideally $\sim$10 Hz) by using mainly information from the Muon Spectrometer, where the occupancy in Pb+Pb is on average lower than in pp, rather than by using the Inner Detector, where the occupancy is high and the reconstruction slow.

8 Perspective for observing heavy-quarkonia decaying into e^+e^-

For the studies with central Pb+Pb collisions, the TRT has not been considered because of its large occupancy. Nevertheless the TRT can be used fully in peripheral collisions, and partially in central ones when selecting inside the TRT in-time signals along the extrapolated trajectory from track reconstruction in the PIXEL and SCT detectors. This should improve tracking and resolution.

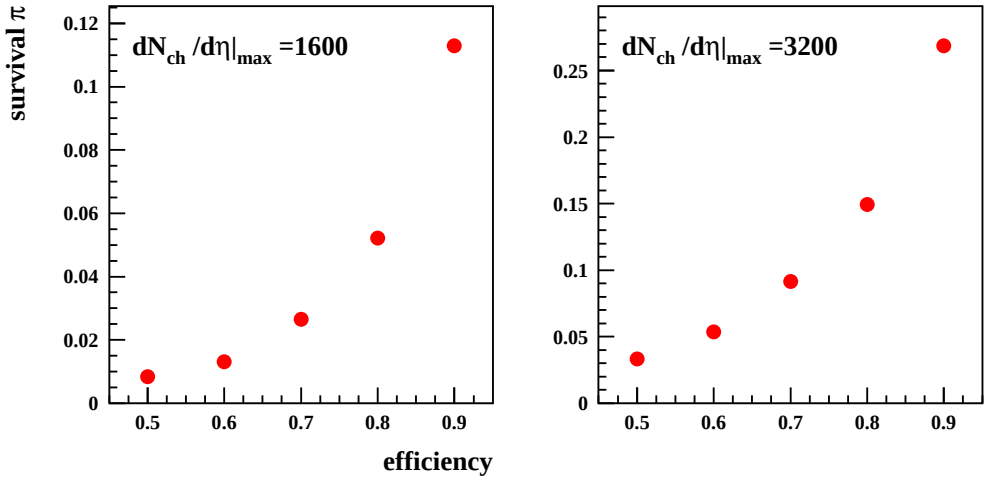

Figure 21: Fraction of survival pions as a function of the electron detection efficiency for a maximum charged particle pseudorapidity density $dN_{ch}/d\eta = 1600$ (left) and 3200 (right).

The TRT can also identify low p_T electrons from Υ and $J/\psi \to e^+e^-$ on a statistical basis without a full reconstruction inside the TRT. A first study is based on the hypothesis that the trajectory of the electron in the TRT can be extrapolated correctly from the track reconstruction, defining so a road where the transition radiation is measured using all signals inside this road. A first evaluation, summarized in Fig. 21, shows the fraction of survival pions as a function of the electron detection efficiency for

two different charged particle densities. A pion rejection factor of 100 can be achieved for an electron efficiency of 50% if the maximum charged particle pseudorapidity density $dN_{ch}/d\eta = 1600$ (left plot) whereas the pion rejection is 30 if the maximum of $dN_{ch}/d\eta = 3200$ (right plot, case of central Pb+Pb collisions). From these plots, one can also deduce that an electron pair detection efficiency of 50% (i.e. an individual electron detection efficiency of 70%) corresponds to a rejection factor against pion pairs of 1600 (120) for respectively a maximum charged particle pseudorapidity density $dN_{ch}/d\eta = 1600$ (3200). We have to consider also the contamination from pion-electron pairs. A more complete evaluation is under way. Thus, the heavy-quarkonia decay into e^+e^- seems promising when limiting the efficiency to 50%, especially in case of a charged particle density lower than expected.

9 Summary

Dissociation of heavy-flavor bosons of the Υ and the J/ψ families is well accessible in heavy-ion collisions with the ATLAS detector. Decays of the resonances into muon pairs were considered. The Υ and Υ' resonances can be measured and separated when limiting the muon acceptance to $|\eta| < 2$. The J/ψ and ψ' can be studied with large statistics using a specially developed muon-tagging algorithm. The background can be reduced to an acceptable level. The choice of selection criteria makes sure that the performance is only slightly affected by the presence of the soft heavy-ion background.

Four different scenarios, including muon-tagging and reduced field in the toroidal magnet of the Muon Spectrometer were studied. Using tagging is basically a trade off between statistics and purity whereas reducing the field is a trade off between statistics and mass resolution. The best compromise between these different strategies depends in large part on the performance of the TRT as a function of the charged multiplicity, which itself is difficult to predict for heavy-ion collisions at the LHC energy.

For the studies with central Pb+Pb collisions, the TRT has not been considered because of its large occupancy. Nevertheless the TRT can be used partially, and even fully in peripheral collisions. This should improve tracking and resolution. The TRT can also identify low p_T electrons from Υ and $J/\psi \rightarrow e^+e^-$. An evaluation is under way.

Another conclusion of these studies is the necessity to trigger on muons with a p_T as low as 3-4 GeV for the Υ and even 1.5 GeV for the J/ψ, a possibility which is under study. A first level trigger using only the ϕ information from the trigger chambers, or the use of a reduced toroidal field could be a solution which is under evaluation.

References

[1] T. Matsui and H. Satz, Phys. Lett. **B178**, 416 (1986).

[2] M.C. Abreu et al.,Phys. Lett. **B410**, 327 (1997).
M.C. Abreu et al.,Phys. Lett. **B410**, 337 (1997).
M.C. Abreu et al.,Phys. Lett. **B450**, 456 (1999).
L. Kluberg, Eur. Phys. J. **C43**, 145 (2005).

[3] A. Adare et al., Phys. Rev. Lett. **98**, 232002 (2007).

[4] N. Brambilla et al., CERN Yellow Report, CERN-2005-005 (2005).

[5] ATLAS Collaboration, the ATLAS Experiment at the CERN Large Hadron Collider, submitted to JINST.
ATLAS Collaboration, ATLAS Detector and Physics Performance, Technical Design Report, CERN/LHCC 99-14.

[6] S. Digal, P. Petreczky, H. Satz, hep-ph/0110406.

[7] F. Abe et al., Phys. Rev. Lett. **75**, 4358 (1995).

[8] D.M. Alde et al., Phys. Rev. Lett. **66**, 133 (1991).

[9] M. Bedjidian et al., hep-ph/0311048.

[10] G. Baur et al., CMS NOTE 2000/060.